





ORIGINAL RESEARCH

Investigation on damping mechanism of machine-side dynamics of permanent magnet synchronous generator-based wind generation system

Xianyu Zhou¹ | Siqi Bu^{1,2,3,4,5,6}  | Bowen Zhou^{7,8}  | Dongsheng Yang^{7,8}  | Lasantha Meegahapola⁹ 

¹Department of Electrical and Electronic Engineering, The Hong Kong Polytechnic University, Kowloon, Hong Kong

²Shenzhen Research Institute, The Hong Kong Polytechnic University, Shenzhen, China

³Research Institute for Smart Energy, The Hong Kong Polytechnic University, Kowloon, Hong Kong

⁴Centre for Grid Modernisation, The Hong Kong Polytechnic University, Kowloon, Hong Kong

⁵International Centre of Urban Energy Nexus, The Hong Kong Polytechnic University, Kowloon, Hong Kong

⁶Centre for Advances in Reliability and Safety, The Hong Kong Polytechnic University, New Territories, Hong Kong

⁷College of Information Science and Engineering, Northeastern University, Shenyang, China

⁸Key Laboratory of Integrated Energy Optimization and Secure Operation of Liaoning Province, Northeastern University, Shenyang, China

⁹School of Engineering, RMIT University, Melbourne, Victoria, Australia

Correspondence

Siqi Bu.

Email: siqi.bu@polyu.edu.hk

Abstract

A permanent magnet synchronous generator-based wind generation system has been predominantly applied in wind farms. With the wide application of wind generation, mechanical shafting attracts wide attention as torsional vibration problems may occur in its mechanical rotational system, which can further affect the power system. The paper first intentionally designs a two-open-loop two-mass shaft subsystem model to investigate the interactions among wind turbine mass, generator mass, and machine-side converter, that is, the machine-side dynamics. Then, a bilateral damping contribution analysis is proposed to investigate the damping mechanism of these machine-side dynamics. The impact mechanism of one dynamic on another through the damping contribution channel can be revealed by modal analysis, indicating the coupling of different oscillation modes and the complex interactions of machine-side dynamics. The established two-open-loop two-mass shaft subsystem model and the proposed bilateral damping contribution analysis with the identified damping contribution channel of the permanent magnet synchronous generator-based wind generation system are validated.

KEYWORDS

damping, oscillations, power system stability, renewable energy sources, wind turbines

1 | INTRODUCTION

Wind power generation has gained widespread adoption globally due to its numerous advantages, such as being clean, environmentally friendly, and recyclable. Among the various

types of wind power generation, the use of permanent magnet synchronous generators (PMSGs) has been rapidly increasing. This is because PMSGs offer a simple structure, low power generation cost, and other benefits compared to different types of generators. As the integration of PMSGs into power

This is an open access article under the terms of the [Creative Commons Attribution-NoDerivs](https://creativecommons.org/licenses/by-nd/4.0/) License, which permits use and distribution in any medium, provided the original work is properly cited and no modifications or adaptations are made.

© 2023 The Authors. *IET Smart Grid* published by John Wiley & Sons Ltd on behalf of The Institution of Engineering and Technology.

systems continues to rise, researchers have been actively investigating the stability analysis of such systems [1, 2].

One key area of focus, as seen in Ref. [3], is the electromechanical interaction between PMSGs and the power system. A reduced PMSG model is proposed in Ref. [4] to study electromechanical oscillation. This model neglects the control loop, which weakly interacts with the power system. Another essential aspect studied in Ref. [5] is the subsynchronous interaction between PMSGs and alternating current networks, especially concerning the sustained power oscillation at subsynchronous frequency observed in Xinjiang Uygur Autonomous Region, China. The authors in Ref. [6] propose a damping controller to deal with subsynchronous interaction in wind integrated power systems. The impact of wind speed variation on subsynchronous oscillation is emphasised in Ref. [7]. The authors in Ref. [8] also verify the efficacy of the proposed damping controller to alleviate the subsynchronous oscillation when considering a three-phase fault. The authors in Refs. [9, 10] analyse the modal interaction among the power system with renewable energy or controllers. There are a lot of modal analysis in Ref. [11] with the application of the participation factors, but none of them focus on the interaction among the machine-side dynamics.

To enhance the small-signal stability of PMSG-based power systems, various strategies have been proposed. For instance, The authors in Ref. [12] present a torque compensation strategy, while the authors in Ref. [13] introduce a new controller for PMSG-based wind turbines. Additionally, researchers have proposed modal shift evaluation in Ref. [14] to quantify the interaction of different modes in power systems integrated with full-converter-based wind power generation.

However, more detailed analyses of PMSGs have revealed the significance of certain oscillation modes that cannot be ignored in mechanical shafting instability [15]. To address this, a multi-mass drive train model has been established in Ref. [16]. Furthermore, the two-mass model is utilised in Ref. [17] to examine the differences between the steady and dynamic states of wind turbine mass and generator mass. The authors in Ref. [18] observe the dynamic performance of PMSGs using the two-mass model. In order to dampen the torsional oscillation of the two-mass model of PMSG, a frequency converter is designed in Ref. [19]. The effectiveness of the two-mass model in analysing the mechanical shafting of the drive train is evident from these studies.

The current study aims to explore the interactions between the multi-mass model of PMSG and the power system, with particular emphasis on the torsional oscillation modes of mechanical shafting and their connections with the electromechanical modes of the power system. While some literature has focused on control methods for two-mass PMSGs that can operate at various speeds [20], others have investigated the interactions between mechanical shafting and the electrical components of the power system [21, 22]. However, there is still a lack of sufficient research on the interaction mechanism in PMSG, particularly concerning the machine-side electromechanical dynamics, including electromechanical and torsional modes. Therefore, this paper aims to fill this research gap by

proposing a novel approach called bilateral damping contribution analysis (BDCA) to uncover the damping mechanism of machine-side dynamics.

The concept of BDCA is derived from the damping torque analysis, which is suitable for large-scale systems and typically applied in the frequency domain [23]. Previous works have successfully utilised damping torque analysis to evaluate subsynchronous torsional interaction in PMSGs with nearby turbine generators [24] and to verify the effectiveness of static synchronous compensator in mitigating subsynchronous resonance (SSR) [25]. Additionally, researchers have studied the damping mechanism of power system stabilizers (PSS) using damping torque analysis [26]. Moreover, a generic implementation framework has been proposed to demonstrate the damping mechanisms of power systems with induction generator-based wind power generation [27]. A novel method has been introduced to investigate the damping contribution from doubly-fed induction generators to the power system [28].

Unlike the traditional damping torque analysis, which mainly focuses on the damping torque's effect on the angular speed, the BDCA approach can provide broader insights into damping contributions, encompassing various oscillation modes. This makes it suitable for evaluating the interactions between the mechanical shaft and electrical components, as well as the interplay between electromechanical and torsional modes in the machine-side dynamics of PMSGs.

This paper presents a comprehensive investigation into the interactions of machine-side dynamics in a PMSG-based wind power generation system. In Ref. [29], a novel two-open-loop two-mass model is developed, allowing for the study of electromechanical dynamics and the demonstration of interactions between different dynamics. In this journal paper, a BDCA is proposed to establish a damping contribution channel, enabling a deeper understanding of the interaction mechanisms within the machine-side dynamics. The main contributions of this research can be summarised as follows: (1) Two-Open-Loop Two-Mass Model: Apart from the established two-open-loop two-mass model in the conference paper, the two-open-loop two-mass model is used to construct the damping contribution channel of the machine-side PMSG, which is further analysed in BDCA. This model offers valuable insights into the interactions between different machine-side dynamics, providing a clearer picture of how these components influence each other. (2) BDCA: The paper introduces a novel approach called BDCA to reveal the damping contribution channel in the system. BDCA is a powerful tool to analyse the interaction of various machine-side dynamics, shedding light on their combined impact on the overall system performance. (3) Modal Analysis and Participation Factors: To further explore the interaction mechanisms, modal analysis is employed to study the damping and frequency variations. Additionally, participation factors are introduced to unveil the contributions of different machine-side dynamics to specific modes, thus confirming the existence and significance of the damping contribution channel.

The subsequent sections of the paper are organised as follows: Section 2 is Modelling and Linearisation. It outlines the process of linearisation and highlights the key

characteristics of the model that make it suitable for studying the interactions of machine-side dynamics. Section 3 is Damping Contribution Analysis. The proposed damping contribution analysis is elaborated in this section. The derivation of the channel's form is thoroughly presented, demonstrating its effectiveness in capturing damping contributions. Section 4 is Case Study. A comprehensive case study is conducted in this section to verify the effectiveness of the proposed damping contribution analysis and the feasibility of the two-open-loop two-mass model. The results provide practical evidence of the damping contribution channel's existence and significance in the overall system dynamics. Section 5 is the Conclusion. The paper concludes with a summary of the findings and contributions. The significance of the developed two-open-loop two-mass model and the damping contribution analysis in understanding the interactions of machine-side dynamics is emphasised. Possible future research directions and applications of the proposed approach are also discussed.

2 | TWO-OPEN-LOOP TWO-MASS SHAFT SUBSYSTEM MODEL

A PMSG connected to the main grid is shown in Figure 1. In order to study the damping contribution channel among machine-side dynamics, the structure of the machine-side dynamics for PMSG is demonstrated in Figure 2, which contains the two-mass shafting model and machine-side converter (MSC). The mechanical shafting of PMSG includes three parts: wind turbine, low-speed drive shaft, and generator. Unlike a doubly fed induction generator (DFIG), there is no gearbox between the wind turbine and generator, which significantly simplifies the structure of PMSG for analysis. Thus, the wind turbine can be regarded as a mass block, and the generator rotor can be regarded as another mass block by using the lumped model [10], which can therefore establish the two-mass model sufficient to describe the mechanical shafting of PMSG and would not miss the corresponding mode when analysing small-signal stability.

A two-open-loop two-mass shaft subsystem model is proposed below to reveal the damping mechanism of machine side dynamics of PMSG and their interacting damping contribution channels.

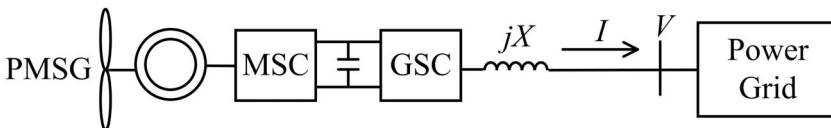


FIGURE 1 A power system integrated with PMSG.

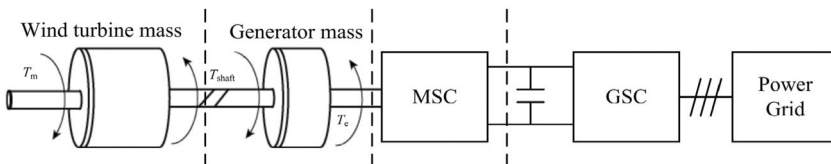


FIGURE 2 A power system with two-mass PMSG.

2.1 | Open-loop subsystem model of wind turbine mass

The linearised state space equation of wind turbine mass can be represented as follows:

$$\Delta \dot{\mathbf{X}}_W = \mathbf{A}_W \Delta \mathbf{X}_W + \mathbf{B}_W \Delta \mathbf{X}_{GM} \quad (1)$$

where $\mathbf{X}_W = [\omega_W \ \delta_W]^T$ is the state variable vector of wind turbine mass, including the angular speed ω_W and the mechanical rotation angle δ_W . $\mathbf{X}_{GM} = [\mathbf{X}_{p2} \ \mathbf{zP}]^T$, where \mathbf{X}_{p2} is the state variable vector of the MSC, $\mathbf{X}_{p2} = [x_{p1} \ x_{p2} \ x_{p3}]^T$, x_{p1} , x_{p2} , x_{p3} are state variables in different control loops of MSC, and \mathbf{zP} is the state variable vector of generator mass, $\mathbf{zP} = [\psi_{psd} \ \psi_{psq} \ \omega_p \ \delta_p]^T$. ψ_{psd} and ψ_{psq} are the direct and quadrature axis flux linkage of the stator winding, ω_p is the angular speed of the generator mass, and δ_p is the mechanical rotation angle of the generator mass. \mathbf{A}_W and \mathbf{B}_W are the corresponding state space matrices.

Equation (1) can be fully represented as

$$\begin{bmatrix} \Delta \dot{\omega}_W \\ \Delta \dot{\delta}_W \end{bmatrix} = \begin{bmatrix} A_{W11} & A_{W12} \\ \omega_{W0} I & 0 \end{bmatrix} \begin{bmatrix} \Delta \omega_W \\ \Delta \delta_W \end{bmatrix} + \begin{bmatrix} B_{W11} & B_{W12} \\ 0 & 0 \end{bmatrix} \begin{bmatrix} \Delta \mathbf{X}_{p2} \\ \Delta \mathbf{zP} \end{bmatrix} \quad (2)$$

2.2 | Open-loop subsystem model of generator mass and MSC

The linearised equation of generator mass and MSC is

$$\Delta \dot{\mathbf{X}}_{GM} = \mathbf{A}_{GM} \Delta \mathbf{X}_{GM} + \mathbf{B}_{GM} \Delta \mathbf{X}_W \quad (3)$$

The above equation can be fully represented as follows:

$$\begin{bmatrix} \Delta \dot{\mathbf{X}}_{p2} \\ \Delta \dot{\mathbf{zP}} \end{bmatrix} = \begin{bmatrix} \mathbf{A}_{GM11} & \mathbf{A}_{GM12} \\ \mathbf{A}_{GM21} & \mathbf{A}_{GM22} \end{bmatrix} \begin{bmatrix} \Delta \mathbf{X}_{p2} \\ \Delta \mathbf{zP} \end{bmatrix} + \begin{bmatrix} \mathbf{B}_{GM1} \\ \mathbf{B}_{GM2} \end{bmatrix} \Delta \mathbf{X}_W \quad (4)$$

where \mathbf{A}_{GM} and \mathbf{B}_{GM} are the corresponding state space matrix.

From Equation (4), the transfer function from different dynamics to wind turbine mass can be calculated.

$$\begin{aligned} Q_z(p) &= \frac{\Delta z p}{\Delta X_w} \\ &= ((p\mathbf{I} - \mathbf{A}_{GM22}) - \mathbf{A}_{GM21}(p\mathbf{I} - \mathbf{A}_{GM11})^{-1} \mathbf{A}_{GM12})^{-1} \\ &\quad \times (\mathbf{B}_{GM2} + \mathbf{A}_{GM21}(p\mathbf{I} - \mathbf{A}_{GM11})^{-1} \mathbf{B}_{GM1}) \end{aligned} \quad (5)$$

$$\begin{aligned} Q_X(p) &= \frac{\Delta X_{p2}}{\Delta X_w} \\ &= ((p\mathbf{I} - \mathbf{A}_{GM11}) - \mathbf{A}_{GM12}(p\mathbf{I} - \mathbf{A}_{GM22})^{-1} \mathbf{A}_{GM21})^{-1} \\ &\quad \times (\mathbf{B}_{GM1} + \mathbf{A}_{GM12}(p\mathbf{I} - \mathbf{A}_{GM22})^{-1} \mathbf{B}_{GM2}) \end{aligned} \quad (6)$$

2.3 | Closed-loop model of machine-side dynamics

The closed-loop model of the whole machine-side dynamics of PMSG is established by integrating the two-open-loop sub-system models together.

$$\begin{bmatrix} \Delta \dot{X}_w \\ \Delta \dot{X}_{GM} \end{bmatrix} = \begin{bmatrix} \mathbf{A}_w & \mathbf{B}_w \\ \mathbf{B}_{GM} & \mathbf{A}_{GM} \end{bmatrix} \begin{bmatrix} \Delta X_w \\ \Delta X_{GM} \end{bmatrix} \quad (7)$$

It can be found that when calculating the statistics of the matrixes in Equation (7), the matrix \mathbf{B}_{w11} is always a 0 matrix, which means that there are no direct dynamic interactions between wind turbine mass and MSC. Then, the closed-loop modes corresponding to wind turbine mass and MSC would not be mutually exclusive when their open-loop modes are coupled [30].

However, in order to find the exact dynamic interactions among machine-side dynamics, the damping contribution channel is established with the assistance of generator mass, which is shown in detail as follows.

The state space equation of MSC represented by state variables of generator mass can be described as follows [12].

$$\Delta \dot{X}_{p2} = \mathbf{A}_{p2} \Delta X_{p2} + \mathbf{B}_{pz} \Delta X_{pz1} \quad (8)$$

where $\Delta X_{pz1} = [\Delta \psi_{psd} \ \Delta \psi_{psq} \ \Delta \omega_p]^T$ is the state variable vector of generator mass directly related to MSC. \mathbf{A}_{p2} and \mathbf{B}_{pz} are the corresponding state space matrix.

Then, it can be obtained from (8) that

$$\Delta X_{pz1} = \mathbf{B}_{pz}^{-1} (p\mathbf{I} - \mathbf{A}_{p2}) \Delta X_{p2} \quad (9)$$

The full representation of Equation (9) is

$$\begin{bmatrix} \Delta \psi_{psd} \\ \Delta \psi_{psq} \\ \Delta \omega_p \end{bmatrix} = \begin{bmatrix} A_{pz11} & A_{pz12} & A_{pz13} \\ A_{pz21} & A_{pz22} & A_{pz23} \\ A_{pz31} & A_{pz32} & A_{pz33} \end{bmatrix} \begin{bmatrix} \Delta x_{p1} \\ \Delta x_{p2} \\ \Delta x_{p3} \end{bmatrix} \quad (10)$$

Thus, the mechanical rotation angle of the generator mass is

$$\Delta \delta_p = \frac{\omega_{p0} I}{p} \Delta \omega_p = \frac{\omega_{p0} I}{p} (A_{pz31} \Delta x_{p1} + A_{pz32} \Delta x_{p2} + A_{pz33} \Delta x_{p3})$$

Then, the relationship between generator mass and MSC can be obtained, that is, the damping contribution channel.

$$\Delta z p = \mathbf{A}_{zz} \Delta X_{p2} \quad (11)$$

where \mathbf{A}_{zz} is the relationship matrix from MSC to generator mass representing the damping contribution channel; it clearly demonstrates the existence of the generator mass damping contribution channel \mathbf{A}_{zz} , which proves that generator mass can act as a channel for MSC to provide damping for wind turbine mass.

Then, the closed-loop model can be represented in Figure 3, in which $\mathbf{G}(p)$ represents the transfer function from generator mass and MSC to wind turbine mass.

3 | BILATERAL DAMPING CONTRIBUTION ANALYSIS OF MACHINE-SIDE DYNAMICS

When analysing the damping contribution channel among machine-side dynamics, consider generator mass and MSC as a whole, which can be seen from the existence of the damping contribution channel to investigate the interactions among machine-side dynamics.

3.1 | BDCA from the generator mass and MSC to wind turbine mass

As has been analysed above, the direct interaction between wind turbine mass and MSC is always 0, and thus the impact of generator mass on wind turbine mass contains two parts, that is, the dynamics of generator mass itself and the dynamics of MSC. Then, in order to study how generator mass and MSC affect the wind turbine mass, $Q_z(p)$ can be differentiated into two parts.

$$Q_{z-z}(p) = (p\mathbf{I} - \mathbf{A}_{GM22}) \times \mathbf{B}_{GM2} \quad (12)$$

$$Q_{z-x}(p) = Q_z(p) - Q_{z-z}(p) \quad (13)$$

where $Q_{z-z}(p)$ and $Q_{z-x}(p)$ represent the transfer function from the dynamics of the generator mass itself and MSC.

Equation (2) can be further transferred into the frequency domain as Figure 4.

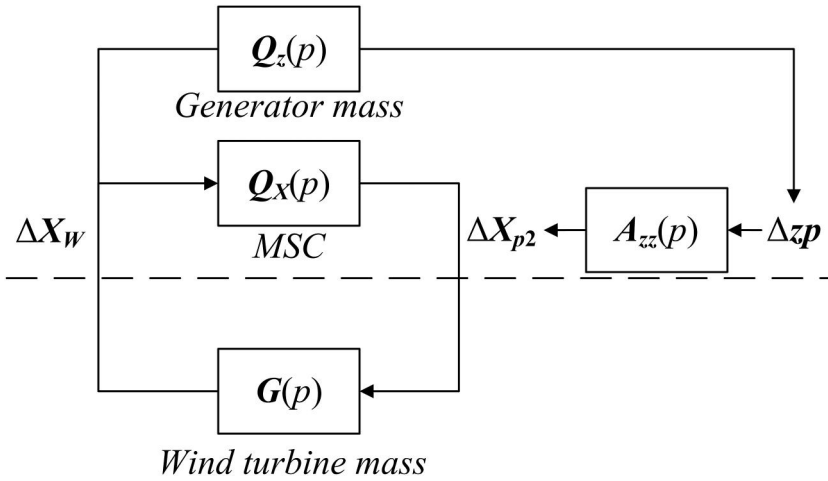


FIGURE 3 Closed-loop model of machine-side dynamics.

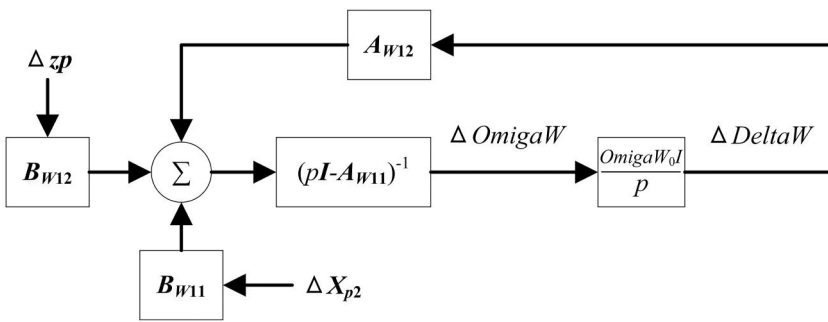


FIGURE 4 Linearised model of wind turbine mass.

The forward path from Δzp and ΔX_{p2} to the electric torque of wind turbine mass is

$$F_z(p) = B_{W12} \quad (14)$$

$$F_x(p) = B_{W11} \quad (15)$$

Assume λ_i is the i th oscillation mode of wind turbine mass, and then ΔX_W should be equal to $\gamma_{iW} \Delta \omega_W$. Thus, it can obtain

$$\begin{aligned} \Delta T_W &= F_z(p) Q_z(p) \Delta zp + F_x(p) Q_x(p) \Delta X_{p2} \\ &= F_z(p) Q_z(p) \Delta zp \end{aligned} \quad (16)$$

$$\Delta X_W = \frac{v_i}{v_{iW}} \Delta \omega_W \quad (17)$$

Thus, $\gamma_{iW} = \frac{v_i}{v_{iW}}$.
Replace p with λ_i ,

$$\begin{aligned} \Delta T_W &= F_z(\lambda_i) Q_z(\lambda_i) \gamma_{iW}(\lambda_i) \Delta \omega_W \\ &= F_z(\lambda_i) Q_{z-z}(\lambda_i) \gamma_{iW}(\lambda_i) \Delta \omega_W \\ &\quad + F_z(\lambda_i) Q_{z-x}(\lambda_i) \gamma_{iW}(\lambda_i) \Delta \omega_W \end{aligned} \quad (18)$$

where $TC_{Wz} = F_z(\lambda_i) Q_{z-z}(\lambda_i) \gamma_{iW}(\lambda_i)$ is defined as the damping torque coefficient of generator mass, and $TC_{Wx} = F_z(\lambda_i)$

$Q_{z-x}(\lambda_i) \gamma_{iW}(\lambda_i)$ is defined as the damping torque coefficient of MSC.

The sensitivity of λ_i with respect to the damping torque coefficient of the mechanical mode of the wind turbine, which refers to the relativity of $\Delta \omega_W$ to λ_i , is shown as follows.

$$S_{iW} = \frac{\partial \lambda_i}{\partial TC_W} = w_{iW} v_{iW} \quad (19)$$

where w_{iW} and v_{iW} are the elements in λ_i associated left eigenvector w_i and right eigenvector v_i corresponding to $\Delta \omega_W$.

Thus, the variation of the i th eigenvalue λ_i in PMSG caused by the dynamics of MSC can be assessed by employing S_{iW} .

$$\begin{aligned} \Delta \lambda_i &= S_{iW} F_z(\lambda_i) Q_{z-z}(\lambda_i) \gamma_{iW}(\lambda_i) \\ &\quad + S_{iW} F_x(\lambda_i) Q_{z-x}(\lambda_i) \gamma_{iW}(\lambda_i) \end{aligned} \quad (20)$$

3.2 | BDCA from wind turbine mass to the generator mass and MSC

The transfer function from generator mass and MSC to wind turbine mass can be obtained from Equation (1).

$$Q_{GM}(p) = \frac{\Delta X_W}{\Delta X_{GM}} = (pI - A_W)^{-1} B_W \quad (21)$$

The full representation of generator mass and MSC can be changed into

$$\begin{bmatrix} \Delta \dot{X}_{\psi x} \\ \Delta \dot{X}_r \end{bmatrix} = \begin{bmatrix} A_{GM11} & A_{GM12} \\ A_{GM21} & A_{GM22} \end{bmatrix} \begin{bmatrix} \Delta X_{\psi x} \\ \Delta X_r \end{bmatrix} + \begin{bmatrix} B_{GM1} \\ B_{GM2} \end{bmatrix} \Delta X_W \quad (22)$$

where $X_{\psi x}$ represents the state variables related to one corresponding mode of generator mass and MSC, and X_r is the remaining variable of X_{GM} .

Equation (22) can also be represented as a similar structure as Figure 5.

Then, the forward path from wind turbine mass to generator mass and MSC can be obtained

$$F_{\psi x}(p) = B_{GM1} + A_{GM12}(pI - A_{GM22})^{-1}B_{GM2} \quad (23)$$

Assume λ_j is the j th oscillation mode of generator mass and MSC, then ΔX_{GM} should be equal to $\gamma_j \Delta X_{\psi x}$, then

$$\gamma_j \Delta X_{\psi x} = \Delta X_{GM} = \frac{v_j}{v_{j\psi x}} \Delta X_{\psi x} \quad (24)$$

Thus, $\gamma_j = \frac{v_j}{v_{j\psi x}}$.

Replace p with λ_j ,

$$\Delta T_{\psi x} = F_{\psi x}(\lambda_j) Q_{GM}(\lambda_j) \gamma_j(\lambda_j) \Delta X_{\psi x} \quad (25)$$

where $T_{C_{\psi x}} = F_{\psi x}(\lambda_j) Q_{GM}(\lambda_j) \gamma_j(\lambda_j)$ is defined as the corresponding damping contribution coefficient.

The sensitivity of λ_j with respect to the damping torque coefficient is shown as follows.

$$S_{j\psi x} = \frac{\partial \lambda_j}{\partial T_{C_{\psi x}}} = w_{j\psi x} v_{j\psi x} \quad (26)$$

where $w_{j\psi x}$ and $v_{j\psi x}$ are the elements in λ_j associated left eigenvector w_j and right eigenvector v_j corresponding to $\Delta X_{\psi x}$.

Thus, the variation of the j th eigenvalue λ_j can be assessed by employing $S_{j\psi x}$.

$$\Delta \lambda_j = S_{j\psi x} F_{\psi x}(\lambda_j) Q_{GM}(\lambda_j) \gamma_j(\lambda_j) \quad (27)$$

4 | CASE STUDY

4.1 | The example power system

The effectiveness of the proposed two-open-loop two-mass model is verified using the system in Figure 1, damping contribution analysis, and the existence of the damping contribution channel. A 15th-order PMSG with synchronous reference frame-phase locked loop dynamics uses the reactive power control with a constant power factor (0.95). The parameters of the example system and controllers of a PMSG in Ref. [31] are used. The control strategies of MSC and grid-side converter (GSC) of PMSG are shown in Figures A1 and A2. The parameters of the mechanical shafting are calculated using the data in Refs. [16, 32].

4.2 | The closed-loop modal analysis

The closed-loop oscillation modes of the machine-side dynamics when the shafting stiffness coefficient $K_{\omega\omega} = 1$ are represented in Table 1; the column of associated variables lists the main participation factors related to corresponding modes. The major participation factors are at least twice that of other participation factors through observed data.

TABLE 1 The closed-loop modes of machine-side dynamics.

No.	$\hat{\lambda}_{wi}$	Frequency (Hz)	Damping ratio	Participation factors
1	$-2.5000 \pm 22.2205i$	3.5365	0.1118	$\Delta\psi_{psd}$
2	$0.0770 \pm 22.4953i$	3.5802	-0.0034	$\Delta\psi_{psq} \Delta x_{p2}$
3	$-2.576 \pm 3.7564i$	0.5979	0.5656	$\Delta\omega_p \Delta x_{p1}$
4	$-0.000 \pm 0.3689i$	0.0587	0.0022	$\Delta\delta_w \Delta\omega_w$
5	-3.5738×10^{-16}	0	1	$\Delta\delta_p$

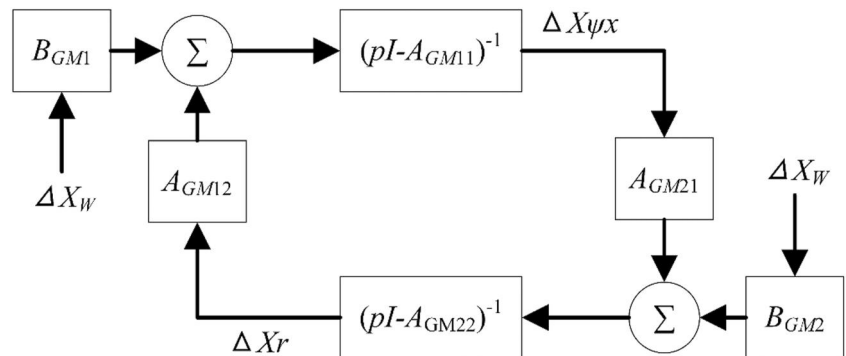


FIGURE 5 Linearised model of generator mass + MSC.

It can be seen that the machine-side dynamics mutually interact with each other, especially the generator mass and MSC, which can be observed from the participation factors of the closed-loop modes, which verifies the feasibility of putting MSC and generator mass together when analysing the damping contribution to wind turbine mass.

The participation factors for wind turbine mass and MSC modes in this condition are shown in Figure 6. The green bar represents the state variables related to wind turbine mass, the red bar represents that of MSC, and the purple bar represents generator mass.

It can be seen that although there is no direct damping contribution from MSC to wind turbine mass, there are some participation factors of MSC existing in the mode of wind turbine mass, which means that there must be a damping contribution channel that assists MSC in having a damping effect on wind turbine mass. The existence of the damping contribution channel will be verified by BDCA, shown as follows.

4.3 | Validation and demonstration of BDCA

4.3.1 | BDCA from generator mass and MSC to wind turbine mass

When wind turbine mass is chosen as the subsystem to analyse damping contribution from generator mass and MSC, the results using BDCA are shown as follows, where the range of shafting stiffness coefficient is calculated according to [33–35]. As the stiffness coefficient is a significant parameter that influences the drive train that connects generator mass and wind turbine mass, the stiffness coefficients of 1, 5, 10, 15, 20, and 25 are taken for analysing the damping contribution analysis in the two-mass shaft model, respectively.

Table 2 shows that, with the increase of shafting stiffness coefficient, the damping contribution from generator mass and MSC to wind turbine mass gets larger, which means the damping contribution channel becomes wider with the increase

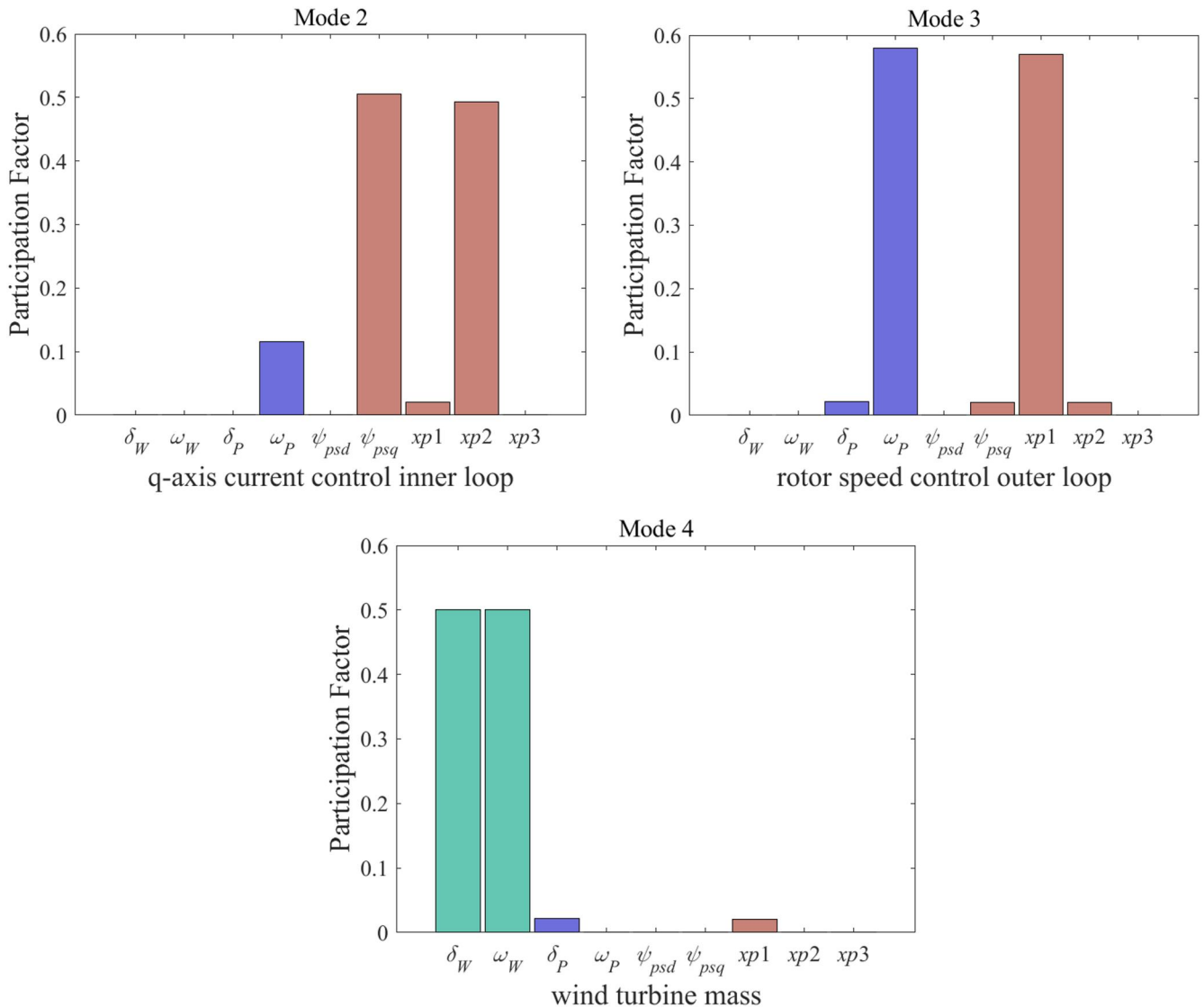


FIGURE 6 The participation factors of wind turbine mass and MSC modes.

TABLE 2 The damping contribution analysis from generator mass and MSC.

K_{ww}	λ_{wi}	$\hat{\lambda}_{wi}$	λ_{Dwi}^a	λ_{Rwi}^b
1	0.0000 + 0.3780i	-0.0008 + 0.3689i	-0.0008 - 0.0090i	-0.0008 - 0.0091i
5	0.0000 + 0.8452i	-0.0146 + 0.7559i	-0.0147 - 0.0843i	-0.0146 - 0.0892i
10	0.0000 + 1.1952i	-0.0411 + 0.9742i	-0.0419 - 0.2000i	-0.0411 - 0.2211i
15	0.0000 + 1.4639i	-0.0682 + 1.1009i	-0.0708 - 0.3175i	-0.0682 - 0.3629i
20	0.0000 + 1.6903i	-0.0926 + 1.1843i	-0.0984 - 0.4312i	-0.0926 - 0.5060i
25	0.0000 + 1.8898i	-0.1138 + 1.2430i	-0.1236 - 0.5399i	-0.1138 - 0.6468i

^a λ_{Dwi} represents the variation calculated by BDCA.

^b λ_{Rwi} represents the real variation between λ_{wi} and $\hat{\lambda}_{wi}$.

TABLE 3 The damping contribution analysis from generator mass and MSC.

K_{ww}	TC_{wz}	TC_{wx}
1	-0.1568 - 0.0834i	0.1552 + 0.0654i
5	-0.4165 - 0.5049i	0.3872 + 0.3362i
10	-0.5181 - 0.9094i	0.4344 + 0.5094i
15	-0.5577 - 1.2270i	0.4161 + 0.5921i
20	-0.5750 - 1.4941i	0.3783 + 0.6317i
25	-0.5819 - 1.7282i	0.3348 + 0.6484i

of stiffness coefficient, resulting in a stronger interaction among machine-side dynamics.

To validate the existence of the damping contribution channel of generator mass from MSC to wind turbine mass, the damping contribution of generator mass and MSC is calculated, respectively, as shown in Table 3. On one hand, it can be seen that the effect of MSC on wind turbine mass is always negative, while the effect of generator mass on wind turbine mass is always positive. Because the damping contribution from generator mass is larger than that of MSC, that is, the damping effect on the wind turbine mass from generator mass suppresses that from MSC, covering the effect of MSC on the wind turbine mass.

On the other hand, the larger the shafting stiffness coefficient, the larger the damping contribution. In this condition, the path from MSC to wind turbine mass through the damping contribution channel of generator mass becomes wider, which can show the importance of stiffness coefficient for the mechanical shaft in the interaction of machine-side dynamics.

In order to further study the interaction of machine-side dynamics, the participation factors of different state variables in the closed-loop oscillation mode of wind turbine mass in different values of shafting stiffness coefficient K_{ww} are shown in Figure 7, where the green bar series represents the state variables related to wind turbine mass, the red bar series represents that of MSC, and the purple bar series represents that of generator mass. For one state variable, the stiffness coefficient increases from left to right. For example, for the state variable x_{p1} , the darkest red bar on the left represents the participation factor where the stiffness coefficient is equal to 1,

the lightest red bar on the right represents the participation factor where the stiffness coefficient is equal to 25, and the middle one represents the participation factor where the stiffness coefficient is equal to 10.

It can be seen that when the value of the stiffness coefficient increases, the participation of generator mass and MSC in the mode of wind turbine mass will also increase, especially the state variables of the rotor speed control outer loop of MSC, which means that when the stiffness coefficient increases, the shaft will become stiffer, the connection between the wind turbine mass and the generator mass will become tighter, and the wind turbine mass will be more easily affected by the damping contribution channel generator mass. Therefore, MSC can have more effect on wind turbine mass through the damping contribution channel in this condition, which is consistent with the damping contribution analysis.

Moreover, it can be observed that the participation of generator mass and MSC is always coupled, which is the same as the result of modal analysis, thus verifying the effectiveness of putting generator mass and MSC together when conducting damping contribution analysis.

4.3.2 | DCA from wind turbine mass to generator mass and MSC

When generator mass and MSC are chosen as the subsystem to analyse the damping contribution from wind turbine mass, the results using DCA are shown as follows. Tables 4–7 show the different modes of the remaining machine-side dynamics affected by wind turbine mass.

Table 4 shows the damping contribution from wind turbine mass to the rotor speed control outer loop of MSC. When the stiffness coefficient gets larger, wind turbine mass can interact with MSC more easily, i.e., the damping contribution channel becomes wider for wind turbine mass.

Table 5 shows that wind turbine mass makes tiny damping to the q -axis current control inner loop of MSC, and with the increase of stiffness coefficient, the interaction among these dynamics becomes larger while far smaller than that of the rotor speed control outer loop.

Table 6 shows that the d -axis current control inner loop of MSC has no interaction with wind turbine mass, no matter what the value of the stiffness coefficient is.

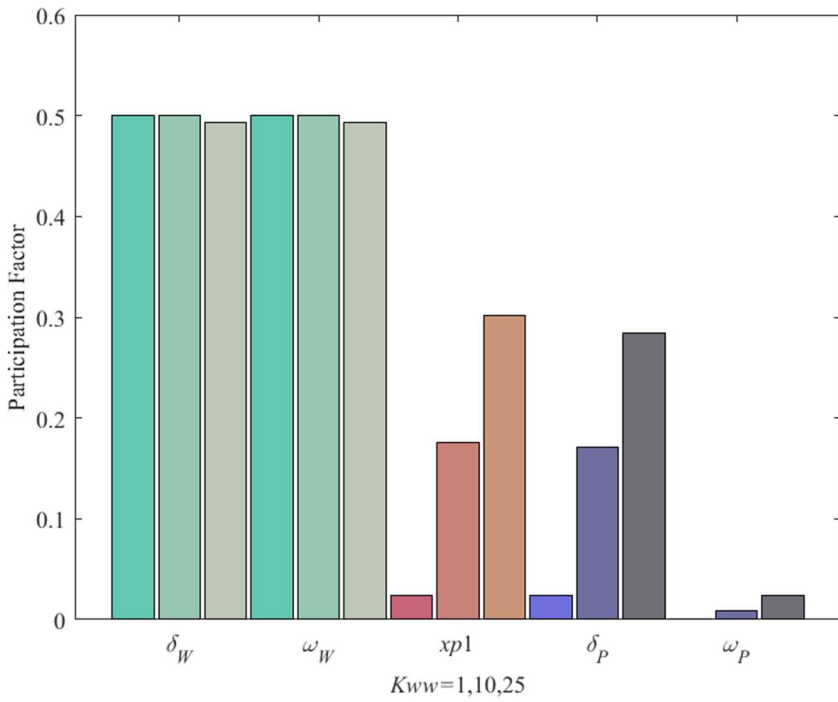


FIGURE 7 The participation of the three parts in different conditions.

K_{ww}	λ_{Roi}	$\hat{\lambda}_{Roi}$	λ_{DRoi}^a	λ_{RRoi}^b
1	$-2.5770 + 3.7561i$	$-2.5762 + 3.7564i$	$0.0008 + 0.0003i$	$0.0008 + 0.0003i$
10	$-2.6222 + 4.7675i$	$-2.5813 + 4.7953i$	$0.0417 + 0.0270i$	$0.0409 + 0.0278i$
25	0	0	0	0

^a λ_{DRoi} represents the variation calculated by BDCA.

^b λ_{RRoi} represents the real variation between λ_{Roi} and $\hat{\lambda}_{Roi}$.

TABLE 4 The damping contribution analysis of the rotor speed control outer loop.

K_{ww}	λ_{qi}	$\hat{\lambda}_{qi}$	λ_{Dqi}^a	λ_{Rqi}^b
1	$0.0770 + 22.4953i$	$0.0770 + 22.4953i$	$0.0000 + 0.0000i$	$0.0000 + 0.0000i$
10	$0.1222 + 22.5092i$	$0.1224 + 22.5092i$	$0.0001 + 0.0000i$	$0.0001 + 0.0000i$
25	$0.2003 + 22.5349i$	$0.2012 + 22.5352i$	$0.0009 + 0.0003i$	$0.0009 + 0.0003i$

^a λ_{Dqi} represents the variation calculated by BDCA.

^b λ_{Rqi} represents the real variation between λ_{qi} and $\hat{\lambda}_{qi}$.

TABLE 5 The damping contribution analysis of the q -axis current control inner loop.

K_{ww}	λ_{di}	$\hat{\lambda}_{di}$	λ_{Ddi}^a	λ_{Rdi}^b
1	$-2.5000 + 22.2205i$	$-2.5000 + 22.2205i$	$0.0000 + 0.0000i$	$0.0000 + 0.0000i$
10	$-2.5000 + 22.2205i$	$-2.5000 + 22.2205i$	$0.0000 + 0.0000i$	$0.0000 + 0.0000i$
25	$-2.5000 + 22.2205i$	$-2.5000 + 22.2205i$	$0.0000 + 0.0000i$	$0.0000 + 0.0000i$

^a λ_{Ddi} represents the variation calculated by BDCA.

^b λ_{Rdi} represents the real variation between λ_{di} and $\hat{\lambda}_{di}$.

TABLE 6 The damping contribution analysis of the d -axis current control inner loop.

K_{ww}	λ_{gi}	$\hat{\lambda}_{gi}$	λ_{Dgi}^a	λ_{Rgi}^b
1	0	0	0	0
10	0	0	0	0
25	$-2.7003 + 0.1121i$	$-2.5874 + 6.0837i$	$0.1129 + 0.1162i$	$0.1226 + 6.1999i$

^a λ_{Dgi} represents the variation calculated by BDCA.

^b λ_{Rgi} represents the real variation between λ_{gi} and $\hat{\lambda}_{gi}$.

TABLE 7 The damping contribution analysis of generator mass.

Table 7 and Figure 8 show that when the stiffness coefficient is small, there is no mode related to generator mass. Because of the coupling of generator mass and MSC, especially the coupling of generator mass and the rotor speed control outer loop, when there is a mode related to the rotor speed control outer loop, the generator mass will have no oscillation mode, and vice versa, which means that when the stiffness coefficient gets more significant to some extent, the mode related to the rotor speed control outer loop may disappear and transfers to the mode of generator mass, which is consistent with Table 4 and verifies the strong coupling of generator mass and MSC and further verifies the correctness of

combining these two dynamics together when analysing damping contribution.

Tables 2–7 can be further presented as Figure 9. It can clearly show that the interaction among machine-side dynamics has the opposite effect on generator mass and MSC with respect to wind turbine mass. The oscillation modes of generator mass and MSC will become deteriorative, while that of wind turbine mass will be improved, and in this situation, the positive/negative damping contributions in the form of complex numbers can be understood as the possible variation of the real part of the eigenvalue is negative/positive, that is, generator mass and MSC can add negative damping to wind

FIGURE 8 The trace of the eigenvalue for generator mass.

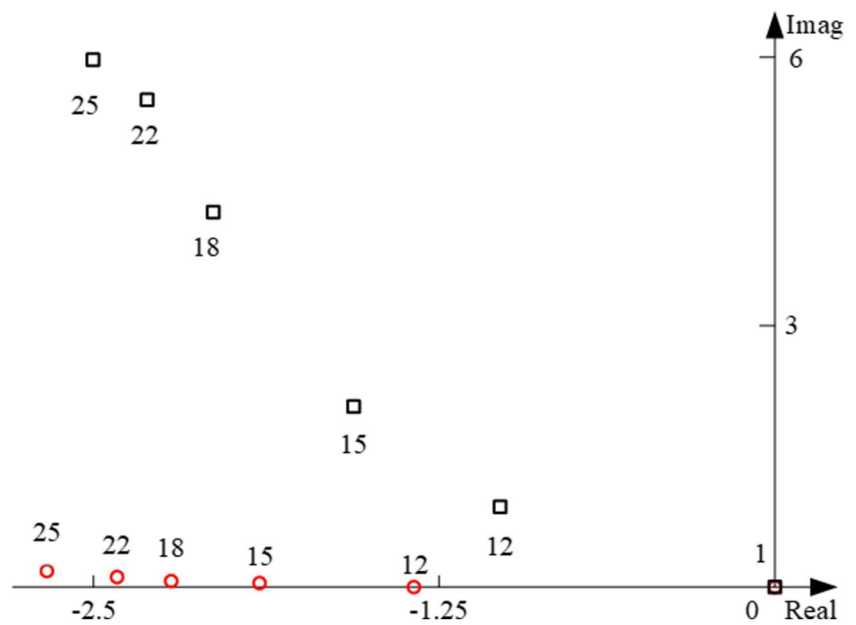
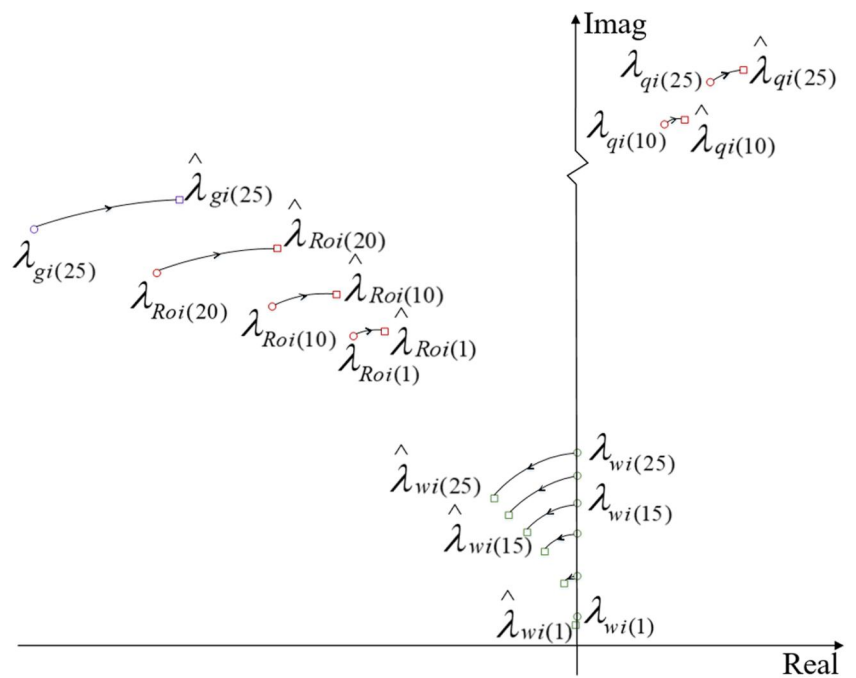


FIGURE 9 Tendency of eigenvalue associated with machine-side dynamics.



turbine mass and can reduce the oscillation frequency, which can improve the oscillation mode; The wind turbine mass would add positive damping to generator mass and MSC and increase the oscillation frequency, which is not beneficial for the stability of MSC and generator mass.

In order to further study the interaction of machine-side dynamics, the participation factors of different state variables in the closed-loop oscillation modes of generator mass and

MSC in different values of shafting stiffness coefficient K_{ww} are shown in Figures 10–11.

It can be seen from Figure 9 that with the increase of stiffness coefficient, the wind turbine mass would participate more in the mode of the rotor speed control outer loop of MSC, which verifies their interaction through the channel of generator mass. It can also be seen that the generator mass and MSC are coupled with each other tightly, and with the increase

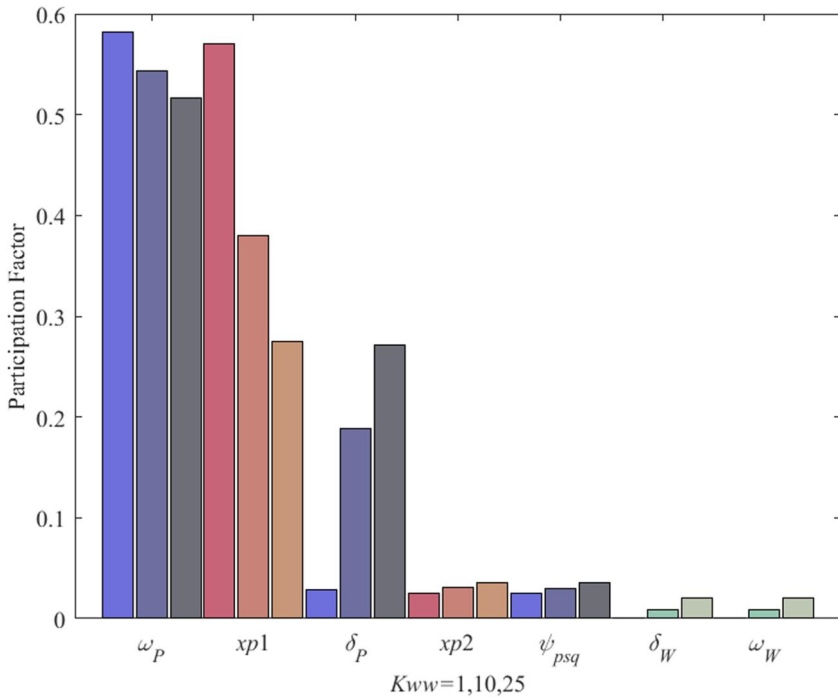


FIGURE 10 The participation factors of rotor speed control outer loop.

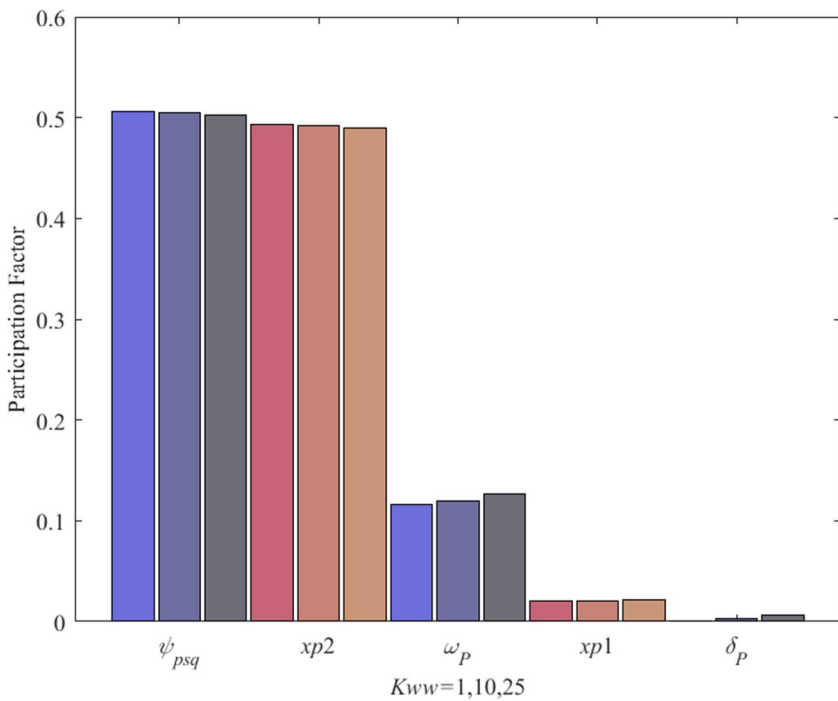


FIGURE 11 The participation factors of the q-axis current control inner loop.

of stiffness coefficient, the generator mass occupies a more significant proportion in this mode, which means the generator mass acts as a more critical channel when the shaft becomes harder.

From Figure 10, it can be seen that the interaction between the q -axis current control inner loop and wind turbine mass hardly changes with the variation of the width of the damping contribution channel, and the participation of wind turbine mass in this mode is non-existent, which means no interaction among machine-side dynamics in the q -axis current control inner loop.

4.4 | Time domain simulations

Time domain simulations are used to verify the effectiveness of the proposed model and damping contribution analysis. A disturbance is performed in the PMSG-based wind generation system (WGS). At $t = 0.2$ s, the wind speed of PMSG is changed, and subsequently, it returns to the same as before the disturbance after 100 ms. The simulation results are shown in Figure 12.

Under the condition of keeping other parameters unchanged, increase the shaft stiffness coefficient K_{ww} from 10 to 25. Figures 12(a–c) illustrate the dynamic performance of power angle and angular speed for wind turbine mass and the point of common coupling voltage.

It can be seen that the oscillatory frequency of wind turbine mass is relatively small, which verifies the results of the modal analysis. Choose the simulation of active power output P_e as an example. As shown in Figure 13, the larger the K_{ww} is, the higher the oscillation frequency and the damping ratio of the output power, which verifies the results of the interaction of machine-side dynamics and further verifies the existence of the damping contribution channel.

5 | DISCUSSION

Based on all the analyses above, some key findings with respect to the damping contribution channel among machine-side dynamics of PMSG-based WGSs are summarised below.

- (1) MSC would not interact with wind turbine mass directly because of their decoupling, which can be observed from the transformation matrix of the closed-loop model. However, it can indirectly interact with wind turbine mass through the damping contribution channel of generator mass;
- (2) The stiffness coefficient is positively related to the oscillation frequency and damping for the coupling modes of generator mass and MSC;
- (3) From the participation factors of the three machine-side dynamics, the rotor speed control outer loop interacts mainly with the wind turbine mass, while the current control inner loop has no interaction with wind turbine mass;

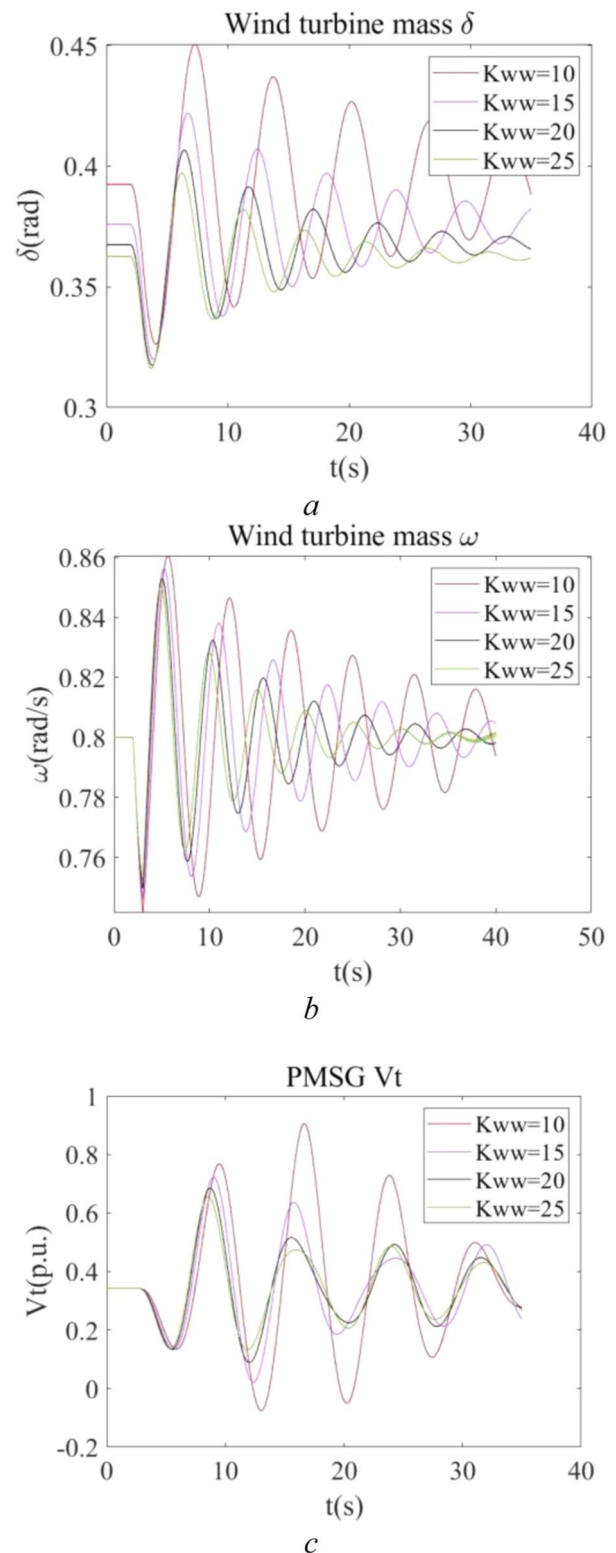


FIGURE 12 The time domain simulation in different stiffness coefficient conditions.

- (4) The interaction of machine-side dynamics will become more significant when the mechanical shafting stiffness coefficient becomes larger as the connection between

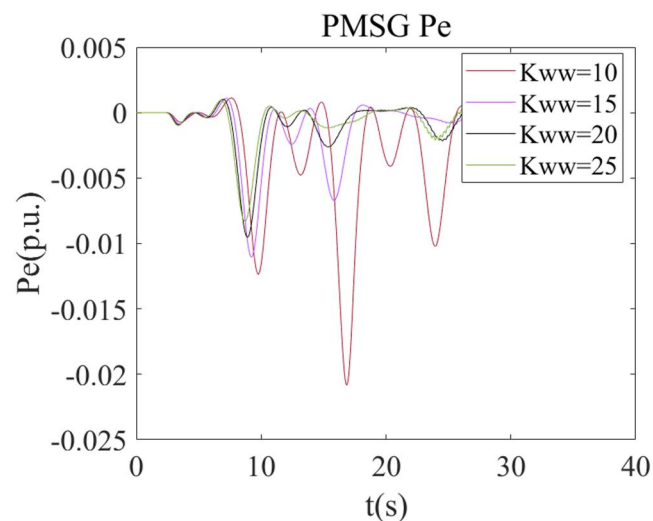


FIGURE 13 Active power response to a small disturbance with different shaft stiffness.

generator mass and wind turbine mass will become tighter, providing a wider damping contribution channel for MSC.

6 | CONCLUSION

The proper understanding of interactions among machine-side dynamics in a PMSG is vital for its efficient operation. As the PMSG is isolated from the power system through a full-power back-to-back converter and the GSC is decoupled from the MSC via the direct current capacitor, the machine-side dynamics stand alone, unaffected by other components. Therefore, it becomes crucial to investigate the interplay between the MSC and the mechanical shaft.

A novel two-open-loop two-mass model is proposed to delve into the intricate interaction of machine-side dynamics in PMSGs. The primary goal is to gain a better understanding of how the MSC and the mechanical shaft influence each other's behaviour. To achieve this, the study utilises damping contribution analysis, complemented by modal analysis, to analyse the response of the system.

The investigation reveals some noteworthy findings:

Indirect interaction through damping contribution channel: Interestingly, the analysis uncovers that there is no direct interaction between the wind turbine mass and the MSC. However, they indirectly influence each other via a damping contribution channel formed by the generator mass. This intricate interaction mechanism highlights the complexity of the PMSG system.

Role of mechanical shaft stiffness coefficient: The study emphasises the pivotal role played by the stiffness coefficient of the mechanical shaft. As this coefficient gains significance, the interaction between the machine-side dynamics intensifies. This effect is attributed to the enhanced integration between the wind turbine mass and the generator mass, allowing the MSC to exert a more pronounced influence on the wind

turbine mass through the broader damping contribution channel.

In conclusion, this paper underscores the importance of investigating the interactions among machine-side dynamics in PMSGs. The proposed two-open-loop two-mass model, along with the damping contribution analysis and modal analysis, offers valuable insights into the subtle interactions between the MSC and the mechanical shaft. Notably, the research sheds light on the impact of the mechanical shaft's stiffness coefficient on the depth and complexity of these interactions. Such a comprehensive understanding holds immense potential for optimising the performance and stability of PMSG-based wind power generation systems.

AUTHOR CONTRIBUTIONS

Xianyu Zhou: Investigation; methodology; software; validation; writing—original draft. **Siqi Bu:** Conceptualisation; funding acquisition; investigation; methodology; project administration; supervision; validation; writing—review and editing. **Bowen Zhou:** Supervision. **Dongsheng Yang:** Supervision. **Lasantha Meegahapola:** Validation.

ACKNOWLEDGEMENTS

The authors would like to acknowledge the support from National Natural Science Foundation of China for the Research Project (52077188).

CONFLICT OF INTEREST STATEMENT


The authors declare no conflicts of interest.

DATA AVAILABILITY STATEMENT

Data sharing is not applicable—no new data is generated.

ORCID

Siqi Bu  <https://orcid.org/0000-0002-1047-2568>

Bowen Zhou  <https://orcid.org/0000-0002-7400-6603>

Dongsheng Yang  <https://orcid.org/0000-0003-1262-5975>

Lasantha Meegahapola  <https://orcid.org/0000-0003-4471-8471>

REFERENCES

- Orlando, N.A., et al.: A survey of control issues in PMSG-based small wind-turbine systems. *IEEE Trans. Ind. Inf.* 9(3), 1211–1221 (2013). <https://doi.org/10.1109/TII.2013.2272888>
- Chen, Q., et al.: Interpretable time-adaptive transient stability assessment based on dual-stage attention mechanism. *IEEE Trans. Power Syst.* 38(3), 2776–2790 (2022). <https://doi.org/10.1109/TPWRS.2022.3184981>
- Du, W., Chen, X., Wang, H.: Power system electromechanical oscillation modes as affected by dynamic interactions from grid-connected PMSGs for wind power generation. *IEEE Trans. Sustain. Energy* 8(3), 1301–1312 (2017). <https://doi.org/10.1109/tste.2017.2677094>
- Li, X., Liao, S., Zha, X.: A reduced-order model of PMSG for the low frequency oscillation analysis of power systems. In: 2019 IEEE Energy Conversion Congress and Exposition (ECCE), pp. 5438–5442. IEEE (2019)
- Liu, H., et al.: Subsynchronous interaction between direct-drive PMSG based wind farms and weak ac networks. *IEEE Trans. Power Syst.* 32(6), 4708–4720 (2017). <https://doi.org/10.1109/TPWRS.2017.2682197>
- Verma, N., et al.: Review of sub-synchronous interaction in wind integrated power systems: classification, challenges, and mitigation techniques.

- Protect. Control Modern Power Syst. 8(1), 17 (2023). <https://doi.org/10.1186/s41601-023-00291-0>
7. Tao, S., et al.: Impedance network model of d-PMSG based wind power generation system considering wind speed variation for sub-synchronous oscillation analysis. *IEEE Access* 8, 114784–114794 (2020). <https://doi.org/10.1109/access.2020.3003754>
 8. Verma, N., Kumar, N., Kumar, R.: Battery energy storage-based system damping controller for alleviating sub-synchronous oscillations in a DFIG-based wind power plant. *Protect. Control Modern Power Syst.* 8(1), 1–18 (2023). <https://doi.org/10.1186/s41601-023-00309-7>
 9. Setiadi, H., et al.: Modal interaction of power systems with high penetration of renewable energy and BES systems. *Int. J. Electr. Power Energy Syst.* 97, 385–395 (2018). <https://doi.org/10.1016/j.ijepes.2017.11.021>
 10. Messina, A.R., Arroyo, J., Barocio, E.: Analysis of modal interaction in power systems with FACTS controllers using normal forms. In: 2003 IEEE Power Engineering Society General Meeting (IEEE Cat. No. 03CH37491), vol. 4, pp. 2111–2117. IEEE (2003)
 11. Shao, B., et al.: Review on power system generalized modal resonance analysis. *Int. J. Electr. Power Energy Syst.* 154, 109417 (2023). <https://doi.org/10.1016/j.ijepes.2023.109417>
 12. Geng, H., Xu, D.: Stability analysis and improvements for variable-speed multipole permanent magnet synchronous generator-based wind energy conversion system. *IEEE Trans. Sustain. Energy* 2(4), 459–467 (2011). <https://doi.org/10.1109/tste.2011.2146285>
 13. Wu, F., Zhang, X.-P., Ju, P.: Small signal stability analysis and control of the wind turbine with the direct-drive permanent magnet generator integrated to the grid. *Elec. Power Syst. Res.* 79(12), 1661–1667 (2009). <https://doi.org/10.1016/j.epsr.2009.07.003>
 14. Luo, J., et al.: Modal shift evaluation and optimization for resonance mechanism investigation and mitigation of power systems integrated with FCWG. *IEEE Trans. Power Syst.* 35(5), 4046–4055 (2020). <https://doi.org/10.1109/tpwrs.2020.2975631>
 15. Salman, S., Teo, A.: Windmill modeling consideration and factors influencing the stability of a grid-connected wind power based embedded generator. *IEEE Trans. Power Syst.* 18(2), 793–802 (2003). <https://doi.org/10.1109/TPWRS.2003.811180>
 16. Liu, J., et al.: Mechanism analysis and suppression strategy research on permanent magnet synchronous generator wind turbine torsional vibration. *ISA Trans.* 92, 118–133 (2019). <https://doi.org/10.1016/j.isatra.2019.02.006>
 17. Xie, D., et al.: Small signal stability analysis for different types of PMSGs connected to the grid. *Renew. Energy* 106, 149–164 (2017). <https://doi.org/10.1016/j.renene.2017.01.021>
 18. Arani, M.F.M., Mohamed, Y.A.-R.I.: Assessment and enhancement of a full-scale PMSG-based wind power generator performance under faults. *IEEE Trans. Energy Convers.* 31(2), 728–739 (2016). <https://doi.org/10.1109/TEC.2016.2526618>
 19. Hansen, A.D., Michalke, G.: Modelling and control of variable-speed multi-pole permanent magnet synchronous generator wind turbine. *Wind Energy Int. J. Progress Appl. Wind Power Convers. Technol.* 11(5), 537–554 (2008). <https://doi.org/10.1002/we.278>
 20. Chen, W., et al.: Control of wide-speed-range operation for a permanent magnet synchronous generator-based wind turbine generator at high wind speeds. *Int. J. Electr. Power Energy Syst.* 136, 107650 (2022). <https://doi.org/10.1016/j.ijepes.2021.107650>
 21. Canay, I.: A novel approach to the torsional interaction and electrical damping of the synchronous machine part 1: theory. *IEEE Trans. Power Apparatus Syst.* PAS-101(10), 3630–3638 (1982). <https://doi.org/10.1109/tpas.1982.317048>
 22. Canay, I.: A novel approach to the torsional interaction and electrical damping of the synchronous machine part 2: application to an arbitrary network. *IEEE Trans. Power Apparatus Syst.* PAS-101(10), 3639–3647 (1982). <https://doi.org/10.1109/tpas.1982.317049>
 23. Hu, Y., et al.: Connection between damping torque analysis and energy flow analysis in damping performance evaluation for electromechanical oscillations in power systems. *J. Modern Power Syst. Clean Energy* 10(1), 19–28 (2021). <https://doi.org/10.35833/mpce.2020.000413>
 24. Muneappa Reddy, J., Rajaram, T., Xu, Y.: Modal analysis on control impact of fully rated converters-based PMSG-WECS connected to turbine-generator. *Elec. Power Compon. Syst.* 49(9–10), 930–942 (2021). <https://doi.org/10.1080/15325008.2022.2049652>
 25. El-Moursi, M.S., Bak-Jensen, B., Abdel-Rahman, M.H.: Novel STATCOM controller for mitigating SSR and damping power system oscillations in a series compensated wind park. *IEEE Trans. Power Electron.* 25(2), 429–441 (2009). <https://doi.org/10.1109/tpe.2009.2026650>
 26. Zhu, X., et al.: Negative damping mechanism analysis of power system stabilizer based on damping torque. *J. Phys. Conf. Ser.* 2320, 012004 (2022)
 27. Bu, S.Q., et al.: Comparison analysis on damping mechanisms of power systems with induction generator based wind power generation. *Int. J. Electr. Power Energy Syst.* 97, 250–261 (2018). <https://doi.org/10.1016/j.ijepes.2017.10.029>
 28. Bu, S., Du, W., Wang, H.: Model validation of DFIGs for power system oscillation stability analysis. *IET Renew. Power Gener.* 11(6), 858–866 (2017). <https://doi.org/10.1049/iet-rpg.2016.0980>
 29. Zhou, X., Bu, S.: Damping torque analysis for mechanical oscillation of PMSG based wind generation system. In: 12th IET International Conference on Advances in Power System Control, Operation and Management (APSCOM 2022), vol. 2022, pp. 182–187. IET (2022)
 30. Du, W., et al.: Concept of modal repulsion for examining the sub-synchronous oscillations in power systems. *IEEE Trans. Power Syst.* 33(4), 4614–4624 (2018). <https://doi.org/10.1109/tpwrs.2018.2790171>
 31. Du, W., Wang, H., Bu, S.: *Small-signal Stability Analysis of Power Systems Integrated with Variable Speed Wind Generators*. Springer (2018)
 32. Akhmatov, V.: Analysis of dynamic behavior of electric power systems with large amount of wind power. Ph.D. Thesis, Ph. D. Dissertation. Technical University of Denmark, Kgs. Lyngby, Denmark (2003)
 33. Ledesma, P., Usaola, J., Rodriguez, J.: Transient stability of a fixed speed wind farm. *Renew. Energy* 28(9), 1341–1355 (2003). [https://doi.org/10.1016/s0960-1481\(02\)00251-3](https://doi.org/10.1016/s0960-1481(02)00251-3)
 34. Trudnowski, D.J., et al.: Fixed-speed wind-generator and wind-park modeling for transient stability studies. *IEEE Trans. Power Syst.* 19(4), 1911–1917 (2004). <https://doi.org/10.1109/tpwrs.2004.836204>
 35. Akhmatov, V., Nielsen, A.H.: Fixed-speed active-stall wind turbines in offshore applications. *Eur. Trans. Electr. Power* 15(1), 1–12 (2005). <https://doi.org/10.1002/etep.29>

How to cite this article: Zhou, X., et al.: Investigation on damping mechanism of machine-side dynamics of permanent magnet synchronous generator-based wind generation system. *IET Smart Grid.* 7(4), 412–426 (2024). <https://doi.org/10.1049/stg2.12145>

APPENDIX

The MSC of PMSG adopts vector control, and its control strategy is shown in Figure A1.

The GSC of PMSG adopts vector control, and its control strategy is shown in Figure A2.

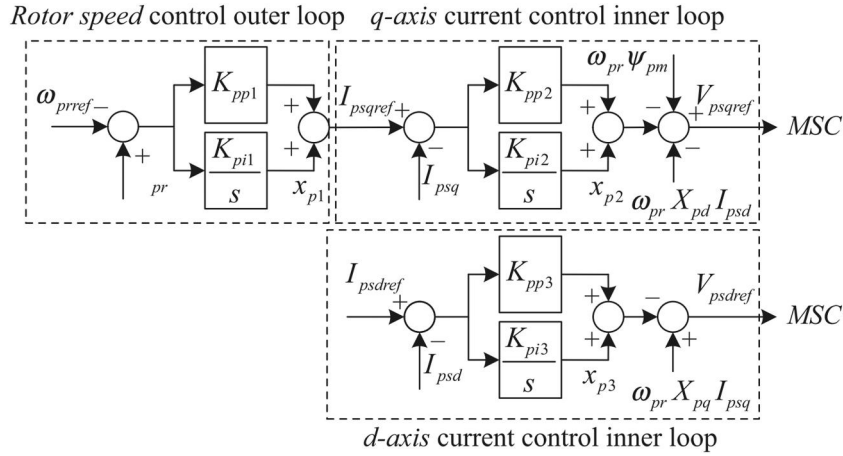


FIGURE A1 Configuration of the control system of the MSC of the PMSG, where K_{pi1} , K_{pi2} , and K_{pi3} are the gains of integral controllers, and K_{pp1} , K_{pp2} , and K_{pp3} are the gains of the proportional controller; for stator windings, X_{pd} and X_{pq} are the d and q -axis reactance. I_{psd} and I_{psq} are the currents of PMSG. I_{psdref} and I_{psqref} are their relevant references. V_{psdref} and V_{psqref} are corresponding terminal voltage references. ω_{pr} is the angular speed of PMSG, and ω_{prref} is the reference of ω_{pr} . Ψ_{pm} is the flux of the permanent magnet.

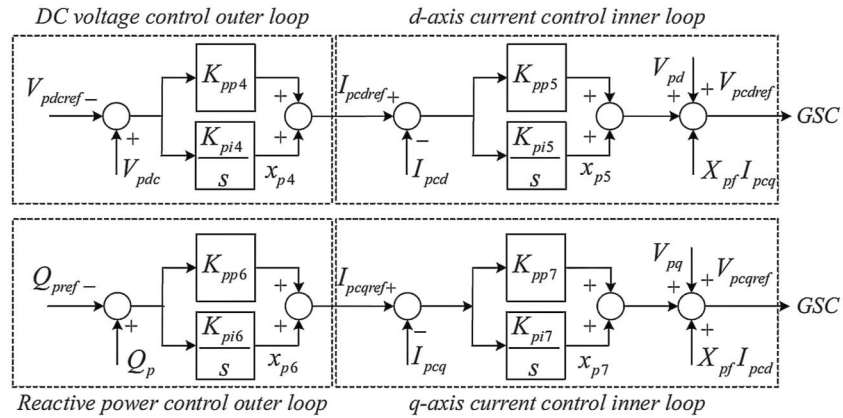


FIGURE A2 Configuration of the control system of the GSC of the PMSG, where I_{pcd} and I_{pcq} are the d and q -axis components of output current from the GSC, respectively; V_{pcd} and V_{pcq} are the references of terminal voltage; V_{pd} and V_{pq} are the voltages of the PCC; V_{pdc} is the DC voltage across the capacitor; Q_{pref} is the reference of the reactive power control outer loop; I_{pcdref} and I_{pcqref} are the references of current control inner loops; V_{pdc} is the reference of the DC voltage control outer loop; Q_p is the reactive power output from the GSC. DC, direct current; PCC, point of common coupling.